pp. 1–13 (2020)

Induced drift of scroll waves in the Aliev–Panfilov model and in an axisymmetric heart left ventricle

S. F. Pravdin*, T. I. Epanchintsev*, T. V. Nezlobinskii*, and A. V. Panfilov*†

Abstract — The low-voltage cardioversion-defibrillation is a modern sparing electrotherapy method for such dangerous heart arrhythmias as paroxysmal tachycardia and fibrillation. In an excitable medium, such arrhythmias relate to appearance of spiral waves of electrical excitation, and the spiral waves are superseded to the electric boundary of the medium in the process of treatment due to high-frequency stimulation from the electrode. In this paper we consider the Aliev–Panfilov myocardial model, which provides a positive tension of three-dimensional scroll waves, and an axisymmetric model of the left ventricle of the human heart. Two relations of anisotropy are considered, namely, isotropy and physiological anisotropy. The periods of stimulation with an apical electrode are found so that the electrode successfully entrains its rhythm in the medium, the spiral wave is superseded to the base of the ventricle, and disappears. The results are compared in two-dimensional and three-dimensional media. The intervals of effective stimulation periods are sufficiently close to each other in the two-dimensional case and in the anatomical model. However, the use of the anatomical model is essential in determination of the time of superseding.

Keywords: Spiral wave, paroxysmal tachycardia, mathematical cardiology, electrotherapy, implantable cardioverter-defibrillator

MSC 2010: 65Z05, 92B25

Rotational modes of electrical excitation in the myocardium are associated with the occurrence of dangerous heart arrhythmias [12]. It is known that rotation can occur around non-excitable areas of the heart, for example, near holes in large vessels or scars after a heart attack [37]. Such an area is called the anatomical block of conducting and serves as the substrate of anatomical reentry. Moreover, the wave can rotate in the absence of an anatomical obstacle, then it is called a spiral wave [41, 42]. In the case of spiral waves, the rotation occurs around the functional core of the wave. The core can be stationary or drift [5, 44]. When the core approaches the electrical boundary of the heart wall, the spiral wave may disappear. Usually, the atrioventricular septum is such boundary in ventricles. Thus, one of the ways to stop an arrhythmia attack is to cause the spiral to drift in the direction of borders of atria and ventricles. It is important that this can be achieved using an external

*Krasovskii Institute of Mathematics and Mechanics, Ural Branch of RAS, Ekaterinburg 620108, Russia; Ural Federal University, HPC Dept., Ekaterinburg 620002, Russia.
E-mail: sfpravdin@imm.uran.ru

†Ghent University, Ghent 9000, Belgium

The work was performed with the use of the ‘URAN’ supercomputer of IMM UB RAS.
The work was supported by the Russian Science Foundation (project No. 17–71–20024).

action with low energy, for example, electrical stimulation with low voltage and current being hundreds of times smaller than in traditional shock cardioversion-defibrillation because the shock defibrillation can damage the heart. This method of electrotherapy is called low-voltage.

One of the methods of low-voltage cardioversion-defibrillation (LVC) is heart stimulation with a period less than the period of arrhythmia [10, 14, 30]. This LVC was studied in a laboratory experiment [31] and in clinic [34, 39] and it demonstrated quite high efficiency, but lesser than shock therapy, i.e., 60% vs. 90%. It is very important to develop LVC methods because shock current pulses damage the myocardium and are extremely painful for conscious patients (this is relevant for atrial arrhythmias) and, when used with implanted cardioverters, their battery is significantly drained.

In excitable media, this LVC method is associated with the drift and superseding of spiral waves [11, 35, 43]. Computer experiment is a very fruitful method for studying LVC and other processes in the heart [2, 4, 22].

We studied LVC in numerical experiments in two-dimensional media using both phenomenological (Aliev–Panfilov [1]) and biophysical (Luo–Rudy LR-I [17], TP06 [36]) models of heart cells and tissue [6, 8, 9, 25, 27]. It turned out that there is an interval of periods that give safe and effective stimulation. In order to compare different models, it is more convenient to specify the boundaries of this interval in fractions of the spiral wave period. For the Aliev–Panfilov model with a discontinuous right-hand side (see Section 1 for parameters), one should use periods from 0.7 to 0.99 [9], for a continuous right-hand side those are periods from 0.8 to 0.99 [27], for the LR-I model those are from 0.9 to 0.99 [6, 8], and for the TR06 model, from 0.95 to 0.99 [25]. At the same time, the degree of anisotropy of the medium and the direction of fibres had little effect on this interval of periods. The size of the electrode and stimulating current in some cases had a significant effect on the results of the process. The role of the latter factor was also pointed out in [33], where the LR-I model was used.

The next step to applying LVC in the clinic is numerical experiments on three-dimensional models of the heart. In this paper we consider an axisymmetric model of the left ventricle (LV) of the human heart [28] as the model contains the least number of parameters, is not related to features of a specific patient, but at the same time it accurately reproduces the form of LV in norm and the directions of muscle fibres in it.

We use the phenomenological cell-level model of Aliev–Panfilov [1] with a discontinuous right-hand side. A spiral wave in this model rotates stably and has a circular core in a flat medium.

A three-dimensional spiral wave rotates around a three-dimensional cylindrical region, the core, which is often represented as a line called a filament. If the filament has the shape of a circle, then the most common type of dynamics is the instability and the drift of the sroll wave, which results in decreasing radius of the circle and annihilation of the vortex [19].

The velocity of this drift has 2 components, the normal one in the plane of

the filament and the binormal component in the orthogonal direction. In the first approximation, the normal component of the drift v_n is described by the equation

$$v_n = b_2 \cdot k$$

where k is the curvature of the thread and b_2 is a coefficient [13]. This equation implies the following equation for filament length ℓ [3]:

$$\frac{\mathrm{d}\ell}{\mathrm{d}t} = -b_2 \int k^2(s)\,\mathrm{d}s.$$

If the filament radius decreases, then the coefficient b_2 is positive and the length of the filament decreases. However, if the filament is not a closed curve, for example, if its ends come out on opposite sides of the parallelepiped, then it takes the form of a straight line orthogonal to the faces, i.e., the line of minimum length [20]. If the thickness of the region is not uniform, then the filament also tends to take the form of a line of minimal length, i.e., it stabilizes at the point of minimal thickness [24]. Note that the above formulas are valid only for a filament of large radius and without torsion and in the absence of anisotropy of the heart tissue. If these factors are present, for example, in an anisotropic case, the curvature of the filament between two faces does not tend to zero, and the filament takes the form of a geodesic in a space whose metric is determined by the anisotropy [40].

A scroll wave in the Aliev–Panfilov model considered here in an isotropic medium of any thickness is also stable and has a straight filament. A spontaneous drift of spiral waves in an isotropic medium was considered in our paper [24]. The method of calculating the tension was proposed in [21]. We used it in [24, 26] and obtained the filament tending to decrease its length and drifting to the domain with a local minimum of depth of the medium. In this paper we study the drift of single scroll waves induced by an external electrical stimulation from a small electrode located in the myocardium. We use various anisotropy ratios and pacing periods. Periods of stimulation demonstrating assimilation of the electrode rhythm, forced drift and disappearance of the spiral wave form a segment. In this paper we study the dependence of the boundaries of that segment on the parameters of the model.

1. Methods

The calculations were performed using monodomain reaction-diffusion equations of the dimensionless Aliev–Panfilov model [1] with two phase variables u and v. Equations and parameters were taken from [26], numerical methods were taken from [29]. Let us present here brief information concerning the model. We solved the system of two equations

$$\frac{\partial u}{\partial t} = \operatorname{div}(D \operatorname{grad} u) - ku(u-a)(u-1) - uv + I_{\mathrm{stim}}(\mathbf{r},t)$$

$$\frac{\partial v}{\partial t} = \varepsilon(u)(ku - v)$$

where $u = u(\mathbf{r},t)$ is the transmembrane potential at the point $\mathbf{r}$ at the time moment t, D is the diffusion matrix, $v = v(\mathbf{r},t)$ is the conductivity for ionic current, $\varepsilon(u) = 1$ for $u < a$, $\varepsilon(u) = \eta$ otherwise, k, a, η are parameters of the model, I_{stim} is the stimulating current. The numerical parameters of the model were $k = 8$, $a = 0.03$, $\eta = 0.1$.

The diffusion matrix D depends on the directions of fibres and diffusion coefficients along fibres D_1 and across fibres D_2. The directions of fibres were obtained with the use of the model of LV of the heart [29] (see Fig. 1c). The LV model uses a special local system of coordinates γ (position from the epicardium $\gamma = \gamma_0$ to the endocardium $\gamma = \gamma_1$), ψ (position from the base $\psi = 0$ to the apex $\psi = \pi/2$), φ (longitude from 0 to 2π).

The LV model has the following parameters: the height from base to apex epicardium of $z_b + h = 60$ mm, the wall thickness at the base of $l = 12$ mm, the outer radius of LV at the base of $r_b + l = 33$ mm, the conicity-ellipticity parameter $\varepsilon = 0.85$, the angle of twist of the spiral surfaces $\varphi_{\max} = 3\pi$, $\gamma_0 = 0.1$, $\gamma_1 = 0.9$ (see details in [29]).

We varied the wall thickness at the apex $h = 6$, 12, 18 mm, the degree of tissue anisotropy, i.e., $D_1 = D_2 = 1$ for isotropy, $D_1 = 1/4$, $D_2 = 1/36$ for physiological anisotropy, stimulation periods P_{stim} from 0.7 to 1.0 relative to the period of spiral wave T_{sw}.

We created a scroll wave using the S1S2 protocol. The first stimulus was applied to the region $0.57 < \psi < 0.62$, $0 \leqslant \varphi < 0.24$, the second one to the region $0 \leqslant \varphi \leqslant \pi$ at the moment of 2160 ms (isotropy), 1960 ms (anisotropy). We observed its spontaneous drift during 40 s and if the wave did not disappear by itself, we repeated the calculations from the beginning adding the electrode stimulation with a certain period from 6 s. The electrode was located in an area $\psi > 1.4$ at the apex of LV (see Fig. 1c). We registered the propagation of plane waves from the electrode and the type of their interactions with the scroll wave.

A spiral wave on a plane has a tip, or center of rotation, and it rotates around the region called the core. Similarly, in a 3-dimensional medium, the tips of a scroll wave form a line called the thread or filament. Based on the results of calculations of the potential u, we found the position of the scroll wave filament using the method described in [26].

The calculation parameters are listed in Table 1, where Δt is the time step, Δr is the effective spatial step. The actual mesh size between grid nodes being uniform in the curvilinear coordinate system, but not uniform in the Cartesian coordinates was withing the range $0.5\Delta r \ldots 2\Delta r$. The scale factors L and T are used to transform the model units (MU) of length and time to mm and ms. We determined them from one-dimensional calculation equating the duration of action potential at the level 90% (APD-90) and the wave velocity to their physiological values from [36]. The stimuli S1 and S2 and stimulation from the electrode were implemented with the use of the current I_{stim} applied during the time period t_{stim}.

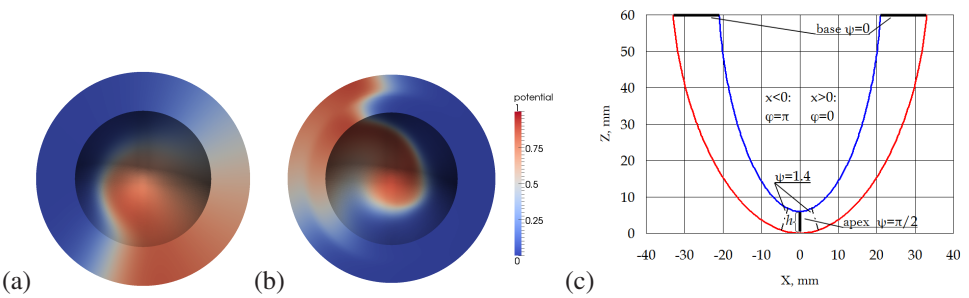

(a) (b) (c)

Figure 1. Model of LV. (a), (b): scroll wave in LV. View from the top. Colour encodes the potential of cells. The apex thickness is $h = 6$ mm. (a): isotropy; (b): anisotropy. (c): cross section of the LV model by vertical plane $y = 0$. Boundaries of the electrode are shown by dash-dotted line.

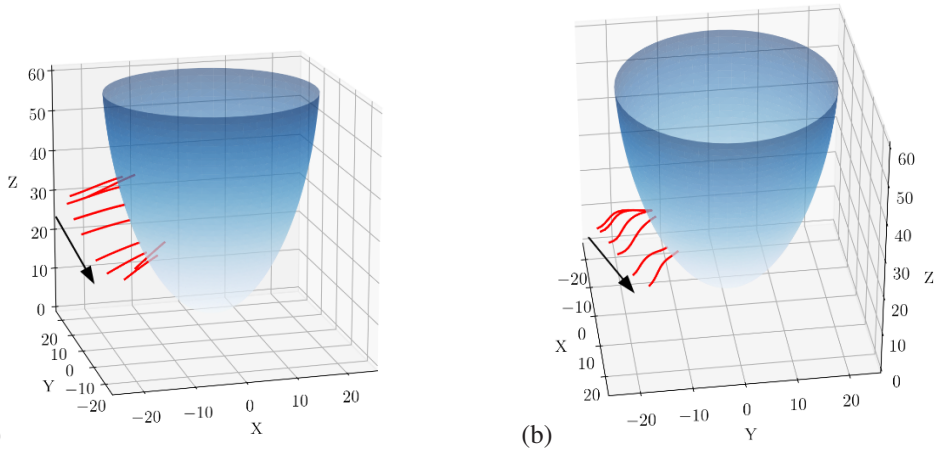

(a) (b)

Figure 2. Filaments of scroll waves in LV. The arrow indicates the direction of drift. The apex thickness is $h = 6$ mm. Blue surface corresponds to endocardium. (a): isotropy; time moments 2.4–2.8 s. (b): anisotropy, time moments 2.3–2.6 s.

Table 1. Parameters of the model and numerical method

Parameter	Isotropy	Anisotropy
Δt, MU	0.01	0.0004
Δt, ms	0.4	0.0016
Δr, mm	1.6	1
L, mm	16	
T, ms	40	
3D T_{sw}, MU	14.4	13.8
3D T_{sw}, ms	576	552
Tension b_2	0.30	
Stimulation current I_{stim}, MU	100	
Duration of stimulation t_{stim}, MU	0.2	

2. Results

2.1. Dynamics of scroll waves without external stimulation

A scroll wave in the LV model is presented in Fig. 1a, b. We see that the anisotropy changes the form of the scroll wave. The beginning of the vortex is near the apex.

Examples of the filaments of scroll waves are presented in Fig. 2. In the model considered here the filament has a positive tension, therefore, it is straight in an isotropic medium. The filament is curved in an anisotropic medium.

It is convenient to describe the dynamics of filaments in the LV model using special coordinates ψ and φ. Figure 3 shows the graph of the coordinates ψ and φ depending on time. If the thickness of the apex is $h = 6$ mm, the wave rotates around the core and around the axis of LV, the degree of anisotropy affects the speed of rotation, i.e., in an anisotropic medium the speed in φ is approximately 3.5 times less than in an isotropic medium. In the isotropic LV for $h = 12$ mm and $h = 18$ mm, the wave disappears after several rotations at the base of LV in approximately 4.5 s ($h = 12$ mm), 7 s ($h = 18$ mm). These data allow us to conclude that the LVC is necessary in the isotropic model only for $h = 6$ mm, and in the anisotropic model in all the considered cases $h = 6$, 12, and 18 mm.

2.2. Effect of external stimulation on the drift of scroll waves

The superseding of a spiral wave passes through 3 consecutive phases [6]: 0 — assimilation of the rhythm by the electrode, 1 — growth of the LV myocardial volume stimulated by the electrode, and displacement of the wave annihilation zone from the electrode and parts of the spiral wave distant from the core towards the core, 2 — forced drift of the spiral wave to the boundary of the medium, in this case, to the base of the ventricle. The graphs show changes in the special coordinate ψ of the filament depending on time (see Fig. 4). The spontaneous drift is replaced by a forced one and the scroll wave approaches the base of LV and disappears there.

An example of a scroll wave during the time of forced drift is presented in Fig. 5.

2.2.1. Isotropy. In this model with the apex thickness of $h = 6$ mm, the spiral wave rotated stably, its filament did not lengthen and did not break up. Applying the stimulation with the periods from 400 ms to 580 ms (i.e., with P_{stim} from 0.69 to 1.01 relative to T_{sw}) with the step 10 ms, we saw that the assimilation of the stimulation and successful superseding were observed for the periods from 430 ms to 520 ms. We did not observe dynamic instability or breakup of the scroll wave caused by external stimulation.

2.2.2. Anisotropy. We found that the minimal periods of successful stimulation are 440 ms ($P_{\text{stim}} = 0.8$) for $h = 6$ mm, 420 ms ($P_{\text{stim}} = 0.76$) for $h = 12$ mm, 400 ms ($P_{\text{stim}} = 0.72$) for $h = 18$ mm. The maximal periods of successful stimulation were 540 ms ($P_{\text{stim}} = 0.97$) for all h. We did not observe any specific features during superseding (dynamic instability, significant elongation of the filament, breakup).

An important parameter of the successful superseding is the time when the spiral wave disappears. It is calculated as the time moment at which the filament searching algorithm stops finding the filament. Graphs of variation of this indicator depending on the stimulation period are presented in Fig. 6 for different periods of stimulation. For convenience of comparing the results for different periods of scroll waves rota-

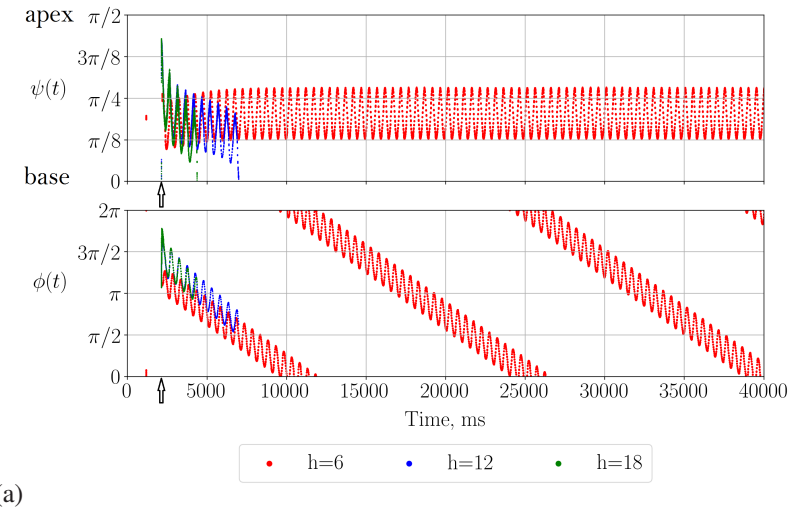

(a)

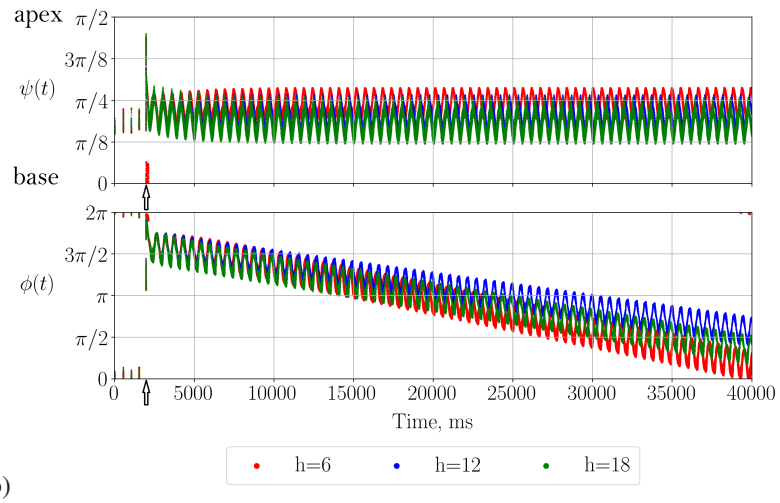

(b)

Figure 3. Dynamics of filaments in LV without external stimulation (spontaneous drift). The apex thickness is $h = 6$, 12, 18 mm. The arrow indicates the moment of applying stimulus S2. (a) isotropy: the period of the spiral is $T_{sw} = 576$ ms. (b) anisotropy: the period of the spiral is $T_{sw} \approx 552$ ms.

tion, we express the periods of stimulation relative to the period of the spiral wave in the given medium, i.e., $P_{stim} = T_{stim}/T_{sw}$.

As seen from the graph in Fig. 6, the time of superseding non-monotonically depends on the stimulation period. This is due to the fact that first several stimuli are not assimilated by the medium. If the rhythm is further assimilated, then the scroll wave is successfully superseded. Otherwise, the Wenckebach effect is observed, every nth stimulus passes, where $n > 1$, and hence the period of waves from the electrode becomes equal to nT_{stim}, which actually exceeds T_{sw} and makes the stimulation ineffective.

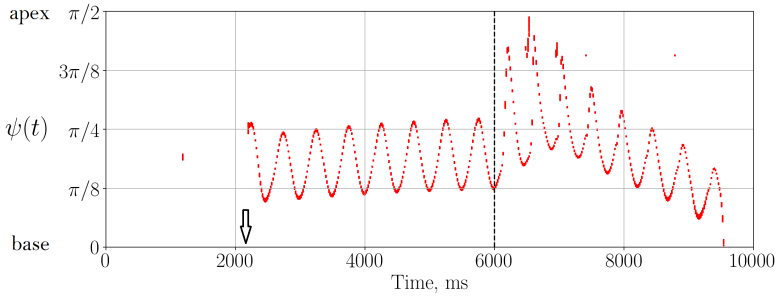

Figure 4. Dynamics of filaments in LV in the presence of external stimulation: variation of coordinate ψ of points of the filament (axis Y) in time (axis X, ms). Until the moment of 6 s we have a slow spontaneous drift of the filament to the apex, between 6 s and 9.5 s we have a fast forced drift to the base of LV and, finally, at the moment 9.5 s the filament disappears. The thickness of the apex is $h = 6$ mm, isotropy. The arrow indicates the moment of applying stimulus S2. The 6 s mark indicates the beginning of the periodic stimulation. The period of stimulation is 460 ms.

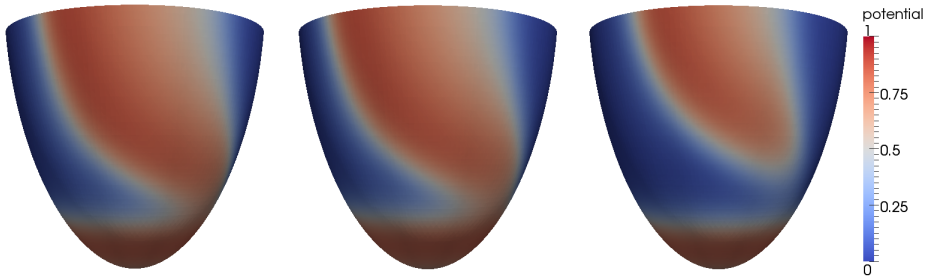

Figure 5. An example of a scroll wave superseded by external source. Anisotropy, the thickness of the apex is $h = 6$ mm, stimulation period is $T_{\text{stim}} = 520$ ms ($P_{\text{stim}} = 0.94$), time moments 10016, 10536, 11056 ms after beginning of the stimulation. The spiral wave is above, the wave from the electrode is below.

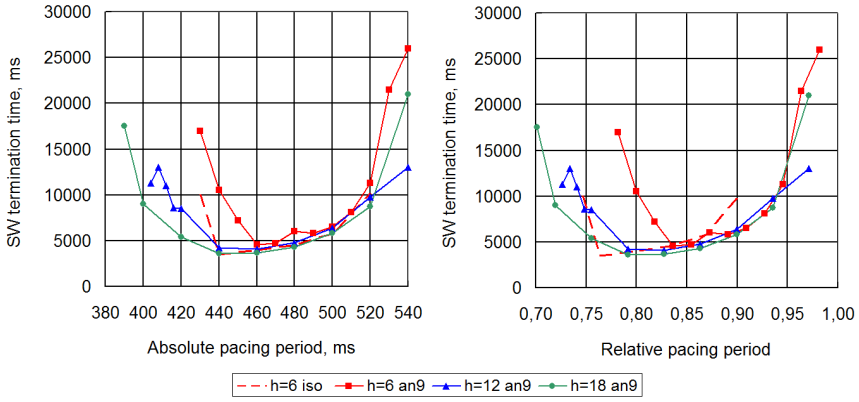

Figure 6. The superseding time of a scroll wave depending on the absolute (left), relative (right) period of stimulation. The moment of the start of stimulation is taken as 0.

Table 2. Periods of successful stimulation.

Medium	Anisotropy ratio	Absolute period, ms		Relative period		T_{sw}, ms
		min	max	min	max	
2D [15]	1	404	572	0.7	0.99	576
2D [9]	9	404	548	0.7	0.95	576
3D	1	430	520	0.75	0.90	576
3D	9	390–430	540	0.7–0.78	0.97	552

3. Discussion and conclusion

Let us consider the obtained boundaries of periods and compare the results of two- and three-dimensional calculations (see Table 2). Considering the minimal and maximal periods, it is more important to determine the first one because it may depend on a variety of factors: cell refractoriness period, minimum diastolic interval, the size of the electrode, the duration and current strength of a single stimulus, and the tendency of waves to dynamic instabilities. At the same time, the maximal period is always slightly less than the period of the spiral wave. If the stimulation period increases, the speed of advance of the zone where the waves from the electrode collide with the scroll wave decreases, therefore, the maximal period is determined by the time that we (and the doctor and patient in the clinic) are willing to wait while the spiral is superseded to the boundary of the medium.

Table 2 shows that the minimal absolute period does not depend on the anisotropy of two-dimensional medium, but it depends on the dimension of the medium and thickness of the heart wall in the three-dimensional anisotropic model. In the most complex case of three-dimensional medium with rotational anisotropy (the last row) the minimal period also depends on the wall thickness at the apex of LV where the electrode is located. The number of nodes for the entire apex of thickness h for all three experiments $h = 6$, 12, and 18 mm was the same and could affect the course of the 0th and 1st phases of the scroll wave superseding (see Subsection 2.2). The qualitative result of stimulation and the speed of forced drift which can be estimated from the time of spiral wave superseding are most dependent on the period of stimulation. This allows us to conclude that two-dimensional calculations are a fairly accurate tool for studying the qualitative characteristics of LVC.

In the case of the same Aliev–Panfilov cell model, the spiral wave superseding time in an anisotropic square was minimal for the minimal assimilated period of stimulation $P_{stim} = 0.7$ [9]. However, we considered previously that in two-dimensional media, the minimal periods should probably be avoided in practice because of the risk of wave breakup and appearance of new spiral waves, which corresponds in the heart to transition from tachycardia to fibrillation being a more dangerous type of arrhythmia. It is advisable to use periods close to the middle of the interval of effective periods. In the three-dimensional medium considered in this paper, this conclusion is also true because the lowest superseding time was observed for average stimulation periods close to $P_{stim} = 0.85$.

The time of the superseding was determined in our paper [25] for ionic cell models. In particular, for the LR-I model [17] in a 100 mm square the superseding

time was less than 10 s [25, Fig. 3]. In this work we observed the superseding time in the range of 5–25 s. Note that the typical path that the contact zone of electrode waves and spiral waves should pass in the case of stimulation from the apex, can be estimated from above as the length of the ventricular arc from the apex to base. In the order of magnitude, it is 100 mm, i.e., close to the superseding path in [25], so the drift speed in the LR-I model is close to the drift speed observed in LV in this paper. The minimal superseding time observed in the LR-I model and in LV in this paper was attained at the same relative stimulation period 0.85–0.90. Note that in the case of anisotropy with circular fibres, the most rapid superseding in the LR-I model was observed with a relative stimulation period of about 0.88–0.9 [7,8]. This type of anisotropy in LV is not studied in this paper.

At the same time, the minimal superseding time in the TP06 model [36] in a 160-mm square was much longer (about 50 s) for the relative stimulation period of 0.97 [25, Fig. 5]. This is due to the fact that the spiral wave period in the TP06 model is close to the refractory period. Therefore, the stimulation with a relative period of 0.85–0.90 was impossible in TP06, but it was most effective in LV in this study.

Realistic three-dimensional modelling of low-voltage defibrillation in atrial arrhythmia [38] has shown that the optimal stimulation period is $P_{\text{stim}} = 0.75 - 0.80$, although other authors report different ranges with a union of 0.69–1.07, and the periods of 0.94–0.95 were effective for all [38, Table 1].

Two-dimensional simulation predicts well the range of periods of successful LVC. Since two-dimensional calculations are performed much faster than three-dimensional ones, the estimation of LVC efficiency can be performed on a two-dimensional medium. However, if we need to calculate the time necessary to stop the arrhythmia, a full three-dimensional modelling is required.

This study did not take into account mechanical processes in the heart, in particular, mechanoelectric feedback. In order to perform such calculations, one can use various software packages such as Chaste [18], Ani3D [16], or LeVen package developed in our group [32]. Such simulation would be interesting and important to conduct in the future because mechanical deformations can affect the dynamics of excitation waves in the myocardium.

Calculation of the spontaneous dynamics of scroll waves with the more realistic T06 cell model [23] has shown that such sources of arrhythmia persist in LV, therefore, some therapy is required, for example, LVC. Further directions of our research in this area will be calculations with biophysical models of heart cells and personalized models of heart ventricles.

References

1. R. R. Aliev and A. V. Panfilov, A simple two-variable model of cardiac excitation. *Chaos, Solitons & Fractals* **7** (1996), 293–301.

2. H. J. Arevalo, F. Vadakkumpadan, E. Guallar, A. Jebb, P. Malamas, K. C. Wu, and N. A. Trayanova, Arrhythmia risk stratification of patients after myocardial infarction using personalized heart models. *Nature Communications* **7** (2016), 11437.

3. V. N. Biktashev, A. V. Holden, and H. Zhang, Tension of organizing filaments of scroll waves.

Philosophical Transactions of the Royal Society of London. Series A: Physical and Engineering Sciences **347** (1994), 611–630.

4. P. M. Boyle, T. Zghaib, S. Zahid, R. L. Ali, D. Deng, W. H. Franceschi, J. B. Hakim, M. J. Murphy, A. Prakosa, S. L. Zimmerman, H. Ashikaga, J. E. Marine, A. Kolandaivelu, S. Nazarian, D. D. Spragg, H. Calkins, and N. A. Trayanova, Computationally guided personalized targeted ablation of persistent atrial fibrillation. *Nature Biomed. Engrg.* **3** (2019), 870–879.
5. I. R. Efimov, V. I. Krinsky, and J. Jalife, Dynamics of rotating vortices in the Beeler–Reuter model of cardiac tissue. *Chaos, Solitons & Fractals* **5** (1995), 513–526.
6. T. Epanchintsev, S. Pravdin, and A. Panfilov, The impact of cardiac tissue anisotropy on spiral wave superseding: A simulation study using ionic cell models. In: *Procedia Computer Science* (Eds. A. Klimova, A. Bilyatdinova, V. Harmandaris, A. Bilas, and A. Boukhanovsky), Vol. 136. Elsevier, 2018, pp. 359–369.
7. T. Epanchintsev, S. Pravdin, and A. Panfilov, Spiral wave drift induced by high-frequency forcing. Parallel simulation in the Luo–Rudy anisotropic model of cardiac tissue. In: *Computational Science — ICCS 2018* (Eds. Y. Shi, H. Fu, Y. Tian, V. V. Krzhizhanovskaya, M. H. Lees, J. Dongarra, and P. M. A. Sloot). Springer Int. Publ., Cham, 2018, pp. 378–391.
8. T. Epanchintsev, S. Pravdin, and A. Panfilov, Simulation of spiral wave superseding in the Luo–Rudy anisotropic model of cardiac tissue with circular-shaped fibres. *J. Comp. Sci.* **32** (2019), 1–11.
9. T. Epanchintsev, S. Pravdin, A. Sozykin, and A. Panfilov, Simulation of overdrive pacing in 2D phenomenological models of anisotropic myocardium. In: *Proc. 6th Int. Young Scientists Conf. in HPC and Simulation YSC 2017* (Eds. A. Klimova, A. Bilyatdinova, J. Kortelainen, and A. Boukhanovsky), Procedia Computer Science, Vol. 119. Elsevier B.V., Kotka, 2017, 245–254.
10. E. A. Ermakova, V. I. Krinsky, A. V. Panfilov, and A. M. Pertsov, Interaction between spiral and flat periodic autowaves in an active medium. *Biofizika* **31** (1986), 318–323 (in Russian).
11. G. Gottwald, A. Pumir, and V. Krinsky, Spiral wave drift induced by stimulating wave trains. *Chaos: An Interdiscip. J. Nonlinear Sci.* **11** (2001), 487–494.
12. J. Jalife, M. Delmar, J. Anumonwo, O. Berenfeld, and J. Kalifa, *Basic Cardiac Electrophysiology for the Clinician*. Wiley-Blackwell, Chichester, 2009.
13. J. P. Keener, The dynamics of three-dimensional scroll waves in excitable media. *Physica D: Nonlinear Phenomena* **31** (1988), 269–276.
14. V. I. Krinsky and K. I. Agladze, Interaction of rotating waves in an active chemical medium. *Physica D: Nonlinear Phenomena* **8** (1983), 50–56.
15. E. Kuklin and S. Pravdin, In-silico analysis of the role of boundary conditions in the induced drift of 2D spiral waves. In: *IEEE 2020 Ural Symp Biomed. Engrg., Radioelectronics and Information Technology (USBEREIT)*. Ekaterinburg, 2020, pp. 81–84.
16. K. Lipnikov, Yu. Vassilevski, A. Danilov et al., *Advanced Numerical Instruments 3D*. https://sourceforge.net/projects/ani3d/.
17. C. H. Luo and Y. Rudy, A model of the ventricular cardiac action potential. Depolarization, repolarization, and their interaction. *Circulation Research* **68** (1991), 1501–1526.
18. G. R. Mirams, C. J. Arthurs, M. O. Bernabeu, R. Bordas, J. Cooper, A. Corrias, Y. Davit, S.-J. Dunn, A. G. Fletcher, D. G. Harvey, M. E. Marsh, J. M. Osborne, P. Pathmanathan, J. Pitt-Francis, J. Southern, N. Zemzemi, and D. J. Gavaghan, Chaste: an open source C++ library for computational physiology and biology. *PLOS Computational Biology* **9** (2013), 1–8.
19. A. Panfilov, A. N. Rudenko, and V. I. Krinsky, Turbulent rings in 3-dimensional active media with diffusion by 2 components. *Biofizika* **31** (1986), 850–854 (in Russian).

20. A. V. Panfilov, R. R. Aliev, and A. V. Mushinsky, An integral invariant for scroll rings in a reaction-diffusion system. *Physica D: Nonlinear Phenomena* **36** (1989), 181–188.

21. A. V. Panfilov and A. N. Rudenko, Two regimes of the scroll ring drift in the three-dimensional active media. *Physica D: Nonlinear Phenomena* **28** (1987), 215–218.

22. A. Prakosa, H. J. Arevalo, D. Deng, P. M. Boyle, P. P. Nikolov, H. Ashikaga, J. J. E. Blauer, E. Ghafoori, C. J. Park, R. C. Blake, F. T. Han, R. S. MacLeod, H. R. Halperin, D. J. Callans, R. Ranjan, J. Chrispin, S. Nazarian, and N. A. Trayanova, Personalized virtual-heart technology for guiding the ablation of infarct-related ventricular tachycardia. *Nature Biomed. Engrg.* **2** (2018), 732–740.

23. S. F. Pravdin, H. Dierckx and A. V. Panfilov, Effect of the form and anisotropy of the left ventricle on the drift of spiral waves. *Biophysics* **62** (2017), 309–311.

24. S. F. Pravdin, H. Dierckx, and A. Panfilov, Drift of scroll waves of electrical excitation in an isotropic model of the cardiac left ventricle. *Russ. J. Numer. Anal. Math. Modelling* **31** (2016), No. 5, 293–304.

25. S. F. Pravdin, T. V. Nezlobinsky, T. I. Epanchintsev, H. Dierckx, and A. V. Panfilov, Simulation of low-voltage cardioversion in a two-dimensional isotropic excitable medium using ionic cell models. In: *Proc. Int. Conf. 'Mathematical Analysis With Applications — In Honor of the 90th Birthday of Constantin Corduneanu' (2018)* (Eds. S. Pinelas, A. Kim, and V. Vlasov), Springer Proc. in Mathematics & Statistics, Vol. 318. Springer, Ekaterinburg, 2020, pp. 273–288.

26. S. F. Pravdin, T. V. Nezlobinsky, and A. V. Panfilov, Inducing drift of spiral waves in 2D isotropic model of myocardium by means of an external stimulation. In: *Proc. 48th Int. Youth School-Conf. 'Modern Problems in Mathematics and its Applications'* (Eds. S. Pravdin and A. Makhnev). IMM UB RAS, Yekaterinburg, 2017, pp. 268–284.

27. S. F. Pravdin, T. V. Nezlobinsky, and A. V. Panfilov, Modelling of low-voltage cardioversion using 2D isotropic models of the cardiac tissue. In: *Proc. Int. Conf. Days on Diffraction 2017* (Eds. O. V. Motygin, A. P. Kiselev, L. I. Goray, T. A. Suslina, A. Ya. Kazakov, and A. S. Kirpichnikova). Saint-Petersburg, 2017, pp. 276–281.

28. S. F. Pravdin, V. I. Berdyshev, A. V. Panfilov, L. B. Katsnelson, O. Solovyova, and V. S. Markhasin, Mathematical model of the anatomy and fibre orientation field of the left ventricle of the heart. *Biomed. Engrg. Online* **54** (2013), 1–21.

29. S. F. Pravdin, H. Dierckx, L. B. Katsnelson, O. Solovyova, V. S. Markhasin, and A.V. Panfilov, Electrical wave propagation in an anisotropic model of the left ventricle based on analytical description of cardiac architecture. *PLOS One* **9** (2014), e93617.

30. C. M. Ripplinger, V. I. Krinsky, V. P. Nikolski, and I. R. Efimov, Mechanisms of unpinning and termination of ventricular tachycardia. *Amer. J. Physiol. Heart Circ. Physiol.* **291** (2006), H184–H192.

31. N. Shaheen, A. Shiti, I. Huber, R. Shinnawi, G. Arbel, A. Gepstein, N. Setter, I. Goldfracht, A. Gruber, S. V. Chorna, and L. Gepstein, Human induced pluripotent stem cell-derived cardiac cell sheets expressing genetically encoded voltage indicator for pharmacological and arrhythmia studies. *Stem Cell Reports* **10** (2018), 1879–1894.

32. A. Sozykin, S. Pravdin et al., LeVen — a parallel system for simulation of the heart left ventricle. In: *Application of Information and Communication Technologies (AICT), 2015 IEEE 9th Int. Conf.*, 2015, pp. 249–252.

33. A. T. Stamp, G. V. Osipov, and J. J. Collins, Suppressing arrhythmias in cardiac models using overdrive pacing and calcium channel blockers. *Chaos: Interdiscip. J. Nonlinear Sci.* **12** (2002), 931–940.

34. M O. Sweeney, Antitachycardia pacing for ventricular tachycardia using implantable cardioverter defibrillators. *Pacing and Clinical Electrophysiology* **27** (2004), 1292–1305.

35. M. Tanaka, M. Horning, H. Kitahata, and K. Yoshikawa, Elimination of a spiral wave pinned at an obstacle by a train of plane waves: Effect of diffusion between obstacles and surrounding media. *Chaos: Interdiscip. J. Nonlinear Sci.* **25** (2015), 103127.

36. K. H. ten Tusscher and A. V. Panfilov, Alternans and spiral breakup in a human ventricular tissue model. *Amer. J. Physiol. Heart Circ. Physiol.* **291** (2006), H1088–1100.

37. S. P. Thomas, A. Thiagalingam, E. Wallace, P. Kovoor, and D. L. Ross, Organization of myocardial activation during ventricular fibrillation after myocardial infarction. *Circulation* **112** (2005), 157–163.

38. L. Uldry, N. Virag, V. Jacquemet, J.-M. Vesin, and L. Kappenberger, Optimizing local capture of atrial fibrillation by rapid pacing: Study of the influence of tissue dynamics. *Annals Biomed. Engrg.* **38** (2010), 3664–3673.

39. M. S. Wathen, P. J. DeGroot, M. O. Sweeney, A. J. Stark, M. F. Otterness, W. O. Adkisson, R. C. Canby, K. Khalighi, C. Machado, D. S. Rubenstein, and K. J. Volosin, Prospective randomized multicenter trial of empirical antitachycardia pacing versus shocks for spontaneous rapid ventricular tachycardia in patients with implantable cardioverter-defibrillators. *Circulation* **110** (2004), 2591–2596.

40. M. Wellner, O.M. Berenfeld, J. Jalife, and A. M. Pertsov, Minimal principle for rotor filaments. *Proc. Natl. Acad. Sci. USA* **99** (2002), 8015–8018.

41. A. T. Winfree and S. H. Strogatz, Organizing centers for three-dimensional chemical waves. *Nature* **311** (1984), 611–615.

42. A. N. Zaikin and A. M. Zhabotinsky, Concentration wave propagation in two-dimensional liquid-phase self-organizing system. *Nature* **225** (1970), 535–537.

43. H. Zhang, B. Hu, and G. Hu, Suppression of spiral waves and spatiotemporal chaos by generating target waves in excitable media. *Phys. Rev. E* **68** (2003), 026134.

44. V. S. Zykov, *Simulation of Wave Processes in Excitable Media*. Manchester Univ. Press, 1987.